iScience

CellPress
OPEN ACCESS

Article

Giant flexoelectric response of uniformly dispersed BT-PVDF composite films induced by SDS-assisted treatment

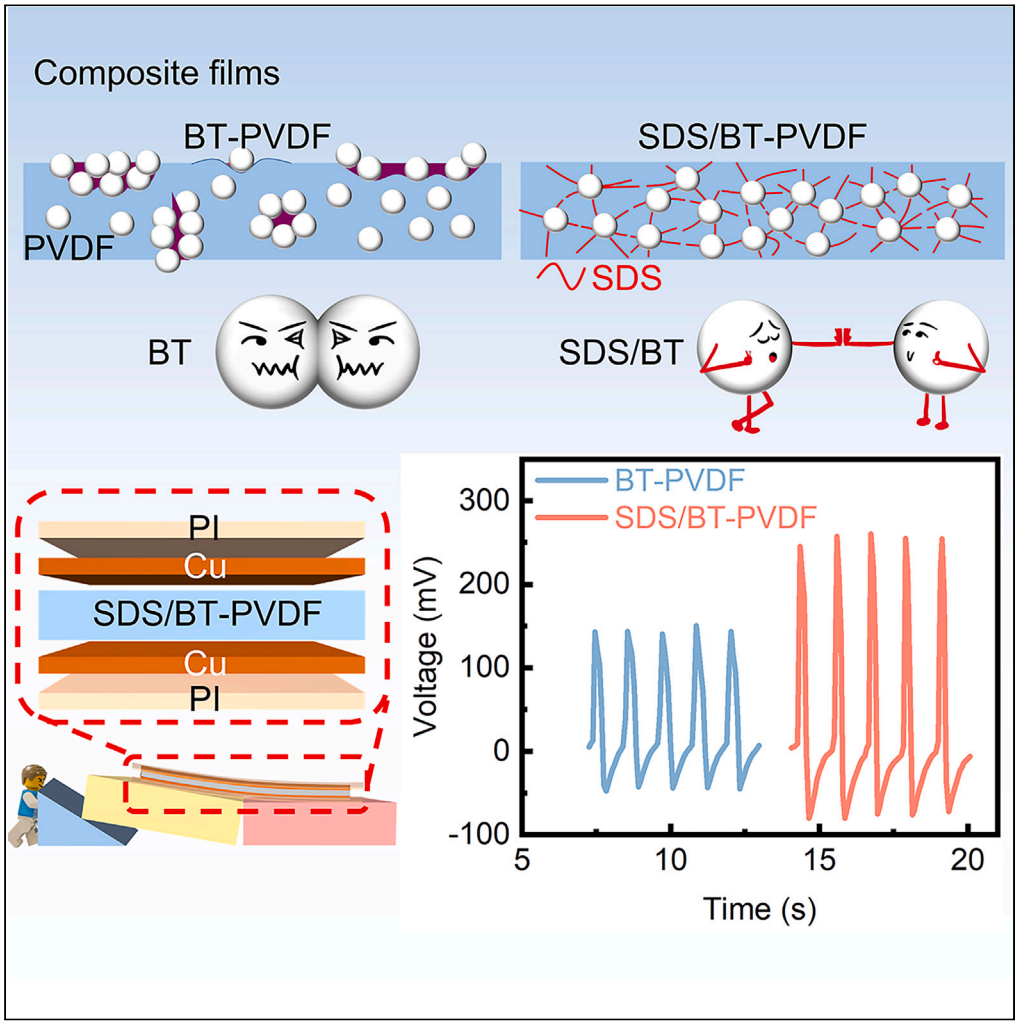

Yujie Wei, Ying Yu, Yuxin Zuo, ..., Hongli Chen, Yang Yang, Chuncheng Zuo

yingyu@zjxu.edu.cn (Y.Y.)
yuxinzuo@zjxu.edu.cn (Y.Z.)

Highlights

A tilt sensor is innovatively prepared based on the flexoelectric response

The uniformly dispersed composite films obtain the giant flexoelectric response

The flexoelectric tilt sensor has high sensitivity and fast response

Wei et al., iScience 26, 107852
October 20, 2023
https://doi.org/10.1016/j.isci.2023.107852

iScience

CellPress
OPEN ACCESS

Article

Giant flexoelectric response of uniformly dispersed BT-PVDF composite films induced by SDS-assisted treatment

Yujie Wei,[1] Ying Yu,[2,5,*] Yuxin Zuo,[3,*] Zhikun Li,[1] Zhiqing Gu,[2] Hongli Chen,[1] Yang Yang,[4] and Chuncheng Zuo[2,4]

SUMMARY

Polymer-ceramic composites are commonly used as flexoelectric films. In existing studies, the flexoelectric effect of composites are generally improved by adjusting the material structures or adding ferroelectric materials. Further improvement of flexoelectric response has encountered a bottleneck. Considering from a new perspective, this study innovatively proposes to prepare the uniformly dispersed BT-PVDF composite films with giant flexoelectric response by surfactant SDS-assisted treatment. According to the engineering applications, tilt sensors have been fabricated with the SDS/BT-PVDF composite films. The prepared tilt sensors can accurately sense the tilt change in a small-angle range (0–10°) between the coaxial connecting parts, the response signal changes significantly (49.25–72.35 mV/°), and the response speed can reach 0.166 s. The research provides a new idea for improving the flexoelectric response and also paves a way for developing tilt sensors through a low-cost, facile, and reliable method, showing potential applications including bending sensing and structural health monitoring.

INTRODUCTION

The flexoelectric effect is an electromechanical coupling between strain gradient and polarization. The bending deformation will induce a strain gradient inside the flexoelectric film and then generate a polarization response.[1–3] The flexoelectric effect has the advantage of "small size,"[4–7] and it is sensitive to the small-scale bending deformation. Polymer films are with excellent flexibility and mechanical reliability, but the flexoelectric response is not significant.[8] Ceramic materials have superior flexoelectric effects, but their brittleness and poor mechanical properties severely limit the further applications in the field of flexible electronics.[9] Existing studies have shown that polymer-ceramic composites prepared by mixing ceramics and polymers could have both excellent flexoelectric effect and mechanical flexibility.[10–12] Studies focusing on the flexoelectric effect are devoted to improving the flexoelectric response of composite films. Scientists tried to increase the flexoelectric response by adding ferroelectric materials, adjusting the structure of materials, and changing the size of the composite.[13–15] The flexoelectric coefficient is an important parameter to characterize the response performance. Research by Huang et al.[16] has pointed out that the flexoelectric coefficient is directly proportional to the dielectric constant of the composite film. Improving the dispersion uniformity of ceramic materials in polymers is an effective means to increase the dielectric constant of the polymer-ceramic composites.[17,18] Therefore, it is reasonable to infer that improving the homogeneity of the ceramic materials in the composites can increase the dielectric constant of the films and then obtain a greater flexoelectric response.

Based on engineering practice, we found that the structural damage caused by the failure of the coaxial connection is often catastrophic in the fields of aerospace, bridges, construction machinery, etc. For example, the tilting of the components at the coaxial joints of the bridge caused by structural aging or damage will lead to collapse accidents.[19,20] In harsh environments, aircraft components are prone to damage such as bolt loosening and cracking, which will threaten the flight safety.[21] It has been realized that real-time monitoring, timely detection, and early diagnosis of the structural damage is an extremely important task. Tilt sensors based on accelerometers, capacitors, gyroscopes, or fiber Bragg grating are commonly used to monitor the tilt angles between the coaxially connected components.[22–26] The accuracies of the accelerometer-based tilt sensors in low and high frequency are 10° and 18°, respectively, and it is difficult to accurately capture the small-angle tilt. Capacitive tilt sensors are more suitable for the measurement of large-angle (<60°) tilt. The fiber Bragg grating tilt sensor can detect the small-angle tilt, but the change of the response signal is not obvious. Methods such as gyroscopes and laser scanning have high precision, but the algorithms are complex and the equipment is cumbersome, making it difficult to achieve real-time monitoring. Because the structural health monitoring of bridges and construction machinery focuses on the tiny tilt, it is crucial to find a method suitable for real-time monitoring of the structural health of coaxial connection components within a small-angle range.[27]

[1]School of Mechanical Engineering, Zhejiang Sci-Tech University, Hangzhou, Zhejiang 310000, China
[2]College of Information Science and Engineering, Jiaxing University, Jiaxing, Zhejiang 314000, China
[3]Jiaxing Nanhu University, Jiaxing 314001, China
[4]School of Mechanical and Aerospace Engineering, Jilin University, Changchun 130000, China
[5]Lead contact
*Correspondence: yingyu@zjxu.edu.cn (Y.Y.), yuxinzuo@zjxu.edu.cn (Y.Z.)
https://doi.org/10.1016/j.isci.2023.107852

Considering the characteristics of the flexoelectric effect and the practical needs of structural health monitoring, we believe that the flexoelectric response could be applied to monitor the small-angle changes of coaxially connected structures. If the flexoelectric film is attached at the junction of the two coaxially connected components, the structural damage caused by the tilt of one of the components will inevitably induce the bending deformation of the flexoelectric film, thus resulting in a polarization response. SDS (sodium dodecyl sulfate) is a commonly used surfactant. Previous studies have shown that the modification of ceramic nanoparticles by SDS can effectively improve the dielectric constant of composite films.[28] Some theoretical studies have also confirmed that the improvement of the flexoelectric effect can be achieved by increasing the dielectric constant of the composites by simulation.[8,29] However, there is no relevant experimental research to establish the relationship between particle dispersion, dielectric constant, and flexoelectric effect clearly at present. This paper innovatively proposes to prepare the uniformly dispersed BT ($BaTiO_3$, barium titanate)-PVDF (polyvinylidene fluoride) composite films induced by SDS-assisted treatment. It is fully confirmed that the particle distribution in the composite film optimized by SDS can improve the dielectric properties and obtain excellent flexoelectric response. Based on engineering applications, tilt sensors sensitive to small-angle tilt would be fabricated by utilizing the SDS/BT-PVDF composite films with giant flexoelectric response. The study will provide new ideas for the application of the flexoelectric response and the development of tilt sensors.

RESULTS

Morphological, structural, and dielectric characterizations

The XRD diffraction peaks of BT and PVDF in Figure 1A are consistent with the studies in Refs.[30,31], fully proving that BT particles are successfully embedded in PVDF with good crystallinity. In addition, the diffraction peaks of SDS/BT-PVDF were almost the same as those of BT-PVDF, indicating that the addition of SDS did not change the crystal phase of the composite.[28] Figures 1B and 1D are the SEM images of BT-PVDF and SDS/BT-PVDF composite films, respectively. Defects (such as pits and cavities) and aggregated BT particles can be clearly seen in the BT-PVDF films. BT particles with high surface binding energies tend to separate from the polymers and aggregate, so multiple defects can be observed on the surface of the BT-PVDF film.[32] However, the SDS/BT-PVDF film has a smooth and even surface with uniform distributions. Figures 1C and 1E show the distribution of Ba element in BT-PVDF and SDS/BT-PVDF composite films. The figures further prove that the addition of SDS effectively promotes the uniform distribution of BT particles. This can be explained by the following two aspects as shown in Figure 1F. Firstly, the SO_4^- of SDS will combine with Ba^+ or Ti^+ of the BT. The adsorption of SDS on the surface of BT particles will reduce the surface energy of BT particles, which could reduce the difference in surface energy between BT and PVDF, thereby optimizing the interface between BT and PVDF. Secondly, the $C_{12}H_{25}OSO_3^-$ groups of SDS will also be adsorbed on the surface of BT particles in the form of micelles, and the electrostatic repulsion between them can effectively avoid the clustering of BT particles.[17,33] The uniform distribution of BT particles in PVDF improves interfacial compatibility. The schematic diagrams are shown in Figures 1G and 1H.

The Zeta potentials of BT and SDS/BT (BT modified by SDS) in DMSO are shown in Figure 2. The results showed that the Zeta potentials of BT and SDS/BT were −18.9 mV and −21.9 mV, respectively. The negative of Zeta potential indicates that the surface of BT nanoparticles is negatively charged. The increase in the absolute value of Zeta potential indicates that the $C_{12}H_{25}OSO_3^-$ groups of SDS have formed micelles on the surface of BT successfully. These groups could enhance the electrostatic repulsion between BT nanoparticles and promote a more uniform dispersion of BT. This further explains the optimized distribution of BT nanoparticles modified by SDS in Figure 1.

The dielectric properties are closely related to the particle distributions in the composite films. It can be seen from Figure 3A that the addition of BT particles makes the composite film obtain a larger dielectric constant at frequencies less than 10^4 Hz. At low frequencies, electrons and ions in the dielectric have sufficient time to shift in response to the changes of the electric field, forming the space-charge polarization. Whereas at high frequencies, the rotational motion (orientation polarization) of the dipolar groups in cured PVDF is extremely difficult, resulting in the prolonged dielectric relaxation. The BT-PVDF film with more defects hinders the space-charge polarization, weakens the polarization response of BT, and further prolongs the dielectric relaxation time. Therefore, as the frequency increases, the dielectric constant decreases and the dielectric loss increases. The addition of surfactant SDS improves the clusters of BT, optimizes the interface between BT and PVDF, reduces film defects, and shortens the dielectric relaxation. This further proves that the main reason for the lower dielectric constant of BT-PVDF is the defects of the film at high frequencies. After adding SDS, the dielectric constant of SDS/BT-PVDF film is significantly improved, which is higher than that of the pure PVDF or BT-PVDF film. From Figure 3B, it can be concluded that the addition of SDS reduces the dielectric loss of the composite films. The dielectric properties of the SDS/BT-PVDF film with uniform particle distributions are better than those of the BT-PVDF film obviously. This conclusion was also confirmed in the study of Mahato et al.[28]

Response characteristics of the composite films

The tests of the response characteristics were based on the cantilever beam method. Coaxially connected building blocks were used to simulate the adjacent components in bridges or other structures as shown in Figure 4A. The prepared tilt sensor was attached above the junction of the two blocks. Then, a tilt angle α was formed between the two blocks as shown in Figure 4B. The response voltage of the tilt sensor was reflected by the KEITHLEY 2450 source meter.

The flexoelectric response performance of the composite films was carried out on the self-built platform. When the tilt angle of the two connected blocks is fixed at 4°, the response voltages V_{p-p} of the composite films are shown in Figure 5A. The V_{p-p} of pure PVDF and BT-PVDF films is about 96 mV and 190 mV, respectively. After modified by SDS, the response voltage V_{p-p} of SDS/BT-PVDF composite film was significantly increased to 335 mV. When a tilt angle is formed between two connected blocks, the composite films will be bent, which will cause the strain gradient in the composite film. The strain gradient forces the symmetrical charge-centers to separate. The positive and negative

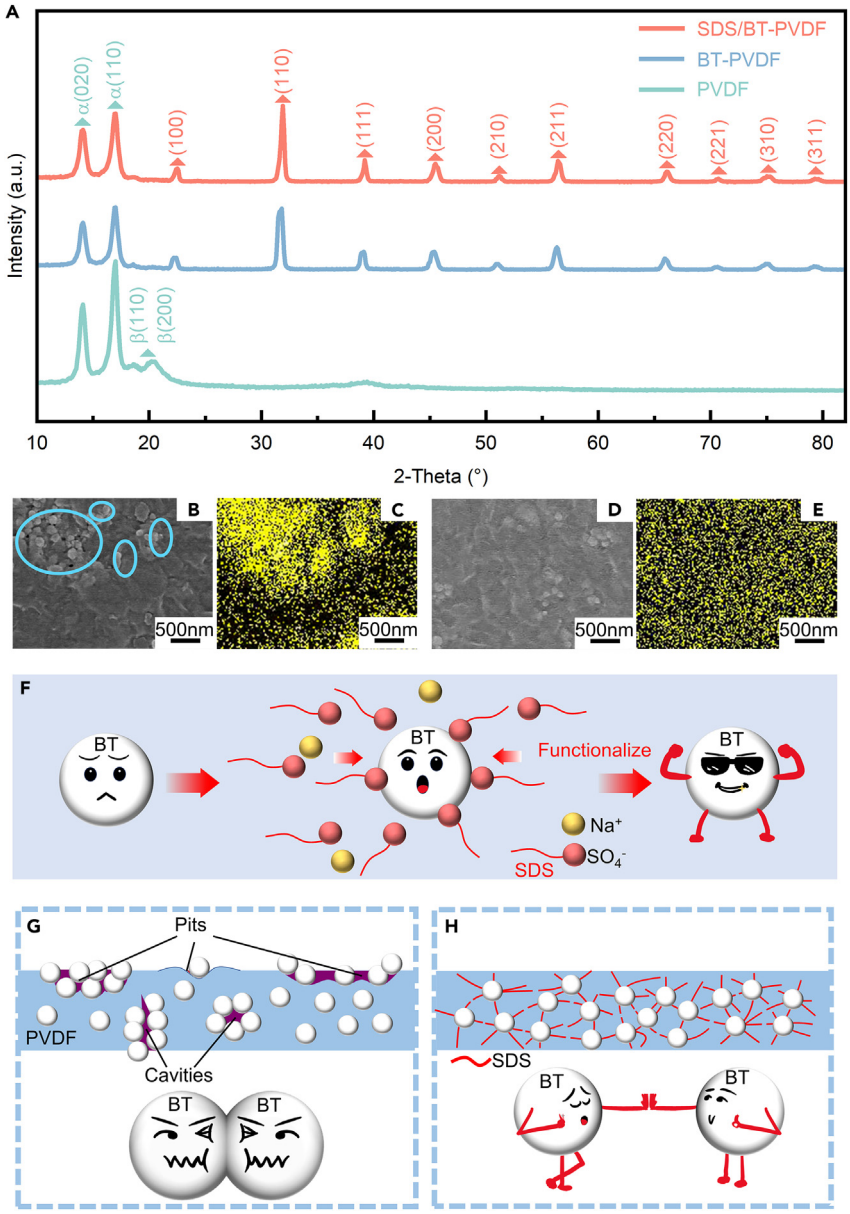

Figure 1. Physical characterization analysis of BT-PVDF and SDS/BT-PVDF

(A) XRD patterns of PVDF, BT-PVDF, and SDS/BT-PVDF films.

(B and C) SEM images and the corresponding EDS elemental mappings of BT-PVDF. Yellow mark is Ba element. Scale bar represents 500 nm.

(D and E) SEM images and the corresponding EDS elemental mappings of SDS/BT-PVDF. Yellow mark is Ba element. Scale bar represents 500 nm.

(F–H) Schematic diagram of the SDS surface modification.

charge-centers move to the two sides of the films respectively. Thus, the flexoelectric response will be generated in the composite films as shown in Figure 5B.

The flexoelectric coefficient is an important parameter to characterize the performance of flexoelectric response. The flexoelectric coefficient μ of the composite film can be calculated based on the cantilever beam model.[34]

$$\mu = \frac{Q\sqrt{1+\left(Slu - \frac{1}{2}Su^2\right)^2}}{A\left(Sl - \frac{1}{2}Su\right)} \quad \text{(Equation 1)}$$

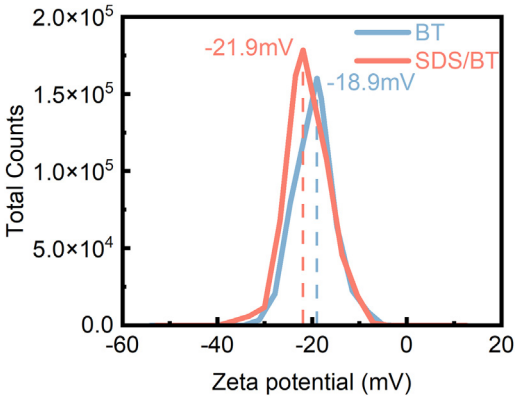

Figure 2. Zeta potential of SDS/BT and BT in DMSO

where Q is the current integral area, u is the effective length, and l is the distance between the fixtures. S can be expressed by the following equation:

$$S = \frac{12y}{l^3} \quad \text{(Equation 2)}$$

where y is the deflection. The flexoelectric coefficients of different films are shown in Figure 5C. The flexoelectric coefficient of pure PVDF and BT-PVDF composite films are 0.13 and 0.55 nC/m, respectively. The SDS/BT-PVDF film has the highest flexoelectric coefficient, which is about 2.11 nC/m. This reflects the same flexoelectric performance as the response voltage shown in Figure 5A. In addition, we found that the flexoelectric coefficient is positively correlated with the permittivity. Taking the frequency of 1 kHz as an example, the relationship between the flexoelectric coefficient and the dielectric constant of the three materials is also clearly reflected in Figure 5C. The flexoelectric coefficient increases with the dielectric constant of the composite films. This fully verified that improving the dielectric properties of materials can effectively improve their flexoelectric effect.[8,29,35]

In order to clarify whether the response signal comes from the flexoelectric effect, we polarized the SDS/BT-PVDF composite film at 70°C with a voltage of 24.5 kV for 35 min. The response voltage of the SDS/BT-PVDF composite film before and after polarization is compared when the bending angle is 10°. As shown in Figure 6, the values of the response voltages of the polarized and unpolarized SDS/BT-PVDF films are almost equal. Polarization can promote the directional arrangement of dipoles in the composite film, and the piezoelectric effect and triboelectric effect of the film will be significantly enhanced after polarization.[36,37] The flexoelectric response originates from the separation of charge-centers caused by the strain gradient and is independent of the orientation of the dipoles. The response voltage of the composite film before and after polarization does not change significantly, which fully proves that the output signal in this study is the response of the flexoelectric effect.

Performance of the tilt sensors

According to the above discussion, the tilt sensor with SDS/BT-PVDF film is taken as the research object, and the sensitivity of the tilt sensor is tested within a small range of 2–10°. Figure 7A shows the response voltage V_{p-p} of the tilt sensor at a frequency of 1 Hz. It can be clearly seen

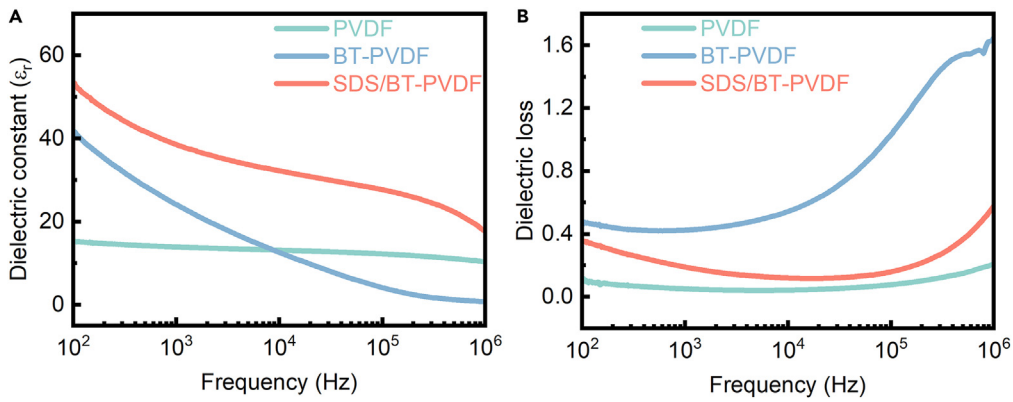

Figure 3. Test of the dielectric performance

(A) Dielectric constant of different composite films.

(B) Dielectric loss of different composite films.

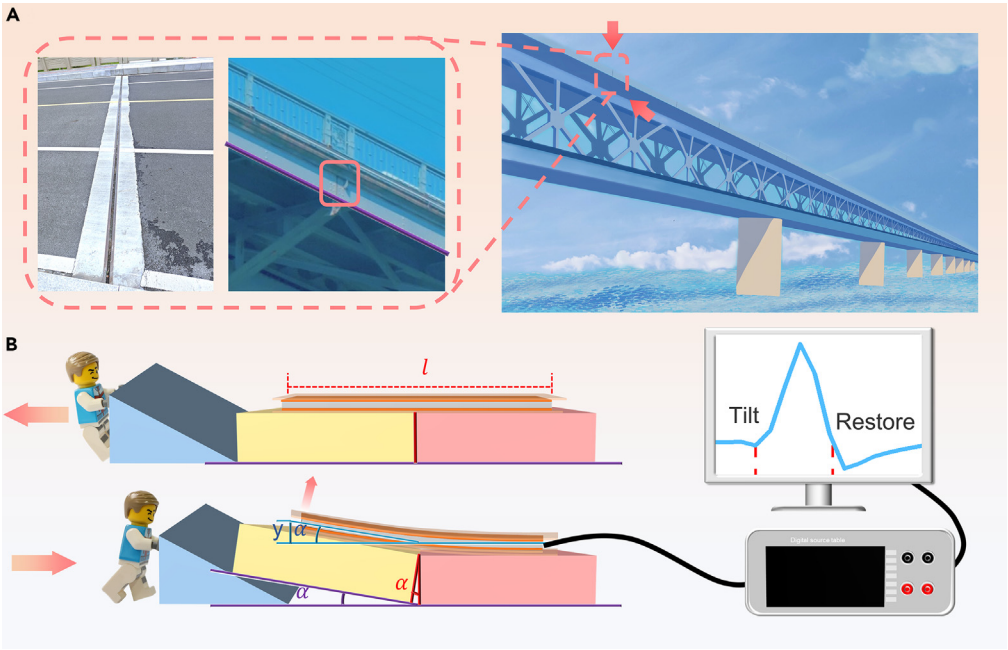

Figure 4. Method for flexoelectric response test

(A) Coaxially connected components in bridges.

(B) Schematic diagram of the structural damage testings.

from the figure that the response voltage increases with the increase of the tilt angle between the two connecting blocks. Therefore, it can be concluded that the tilt sensor has good sensitivity and can recognize the tilt angle accurately according to the magnitude of the response voltage. The bending strain gradient caused by different tilt angles makes the sensor generate different polarization responses. The strain gradient increases as the tilt angle increases, so the flexoelectric response voltage will also increase. The relationship among the bending

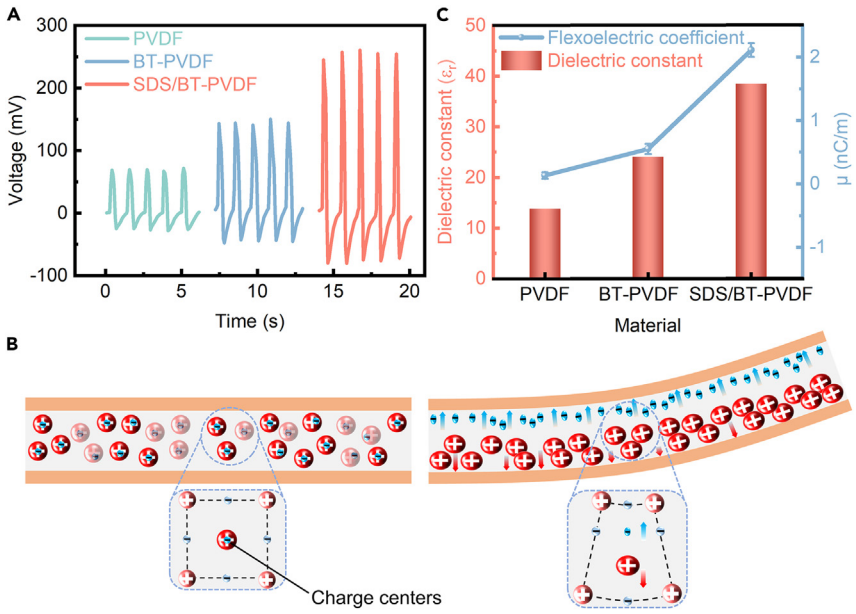

Figure 5. Performance and mechanism of flexoelectric response

(A) Comparisons of flexoelectric responses of the composite films.

(B) Schematic of the flexoelectric response.

(C) The dielectric constant and the flexoelectric coefficient of different composite films. Data are represented as mean ± SEM.

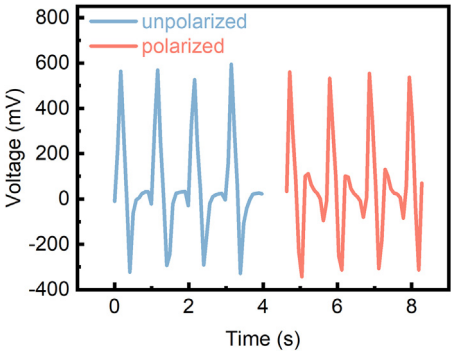

Figure 6. The response voltage of the SDS/BT-PVDF composite film before and after polarization

strain gradient, response voltages, and the tilt angle is shown in Figure 7B. The response time of the tilt sensor is shown in Figure 7C. When different tilt angles are formed between the connecting blocks, the response signal changes significantly (49.25–72.35 mV/°), and the response speed can reach 0.166 s. Compared with the existing studies about sensors based on flexoelectric effect, the response time of the prepared tilt sensor in this study has obvious advantages.[38,39]

In addition, the tilt sensors used to monitor the structural health should have excellent sensitivity and durability. The performance of the tilt sensor has been verified by detecting the continuous damage to the coaxial blocks at different tilt angles with the frequency of 1 Hz. Figure 8 shows the response voltage of the tilt sensor when the tilt changes continuously for 3000 s. It can be seen from the figure that the voltages of the tilt sensors respond obviously to different tilt angles. This fully proves that the sensors have excellent sensitivity and can accurately reflect

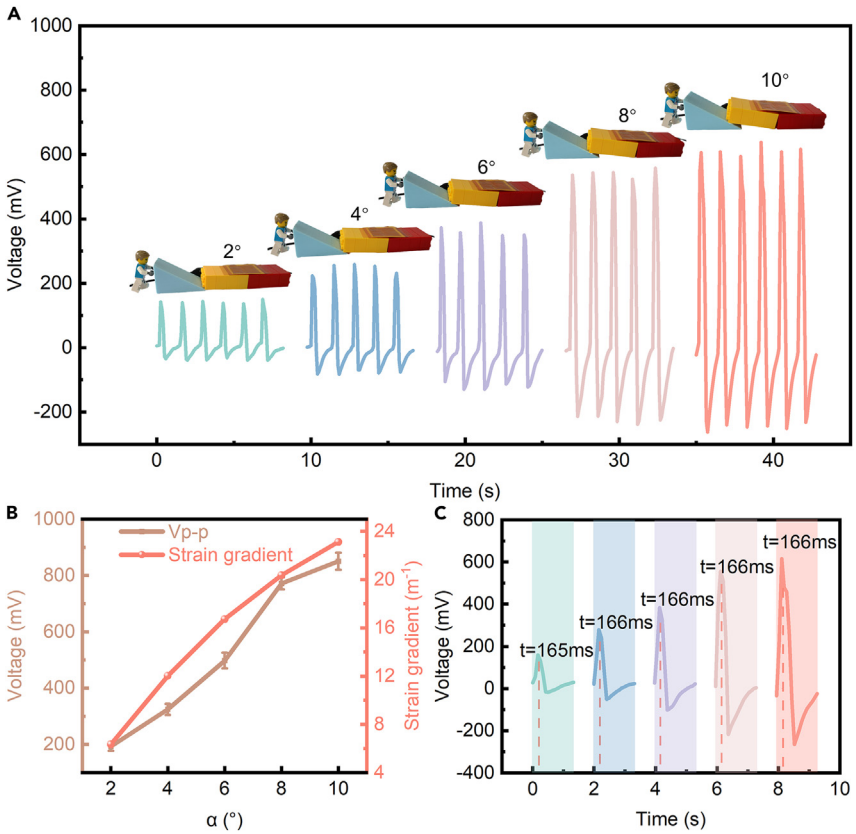

Figure 7. Tilt sensor performance test

(A) Flexoelectric responses at different tilt angles.

(B) The effects of the tilt angles on the strain gradients and the response voltages. Data are represented as mean ± SEM.

(C) The response time of the tilt sensors.

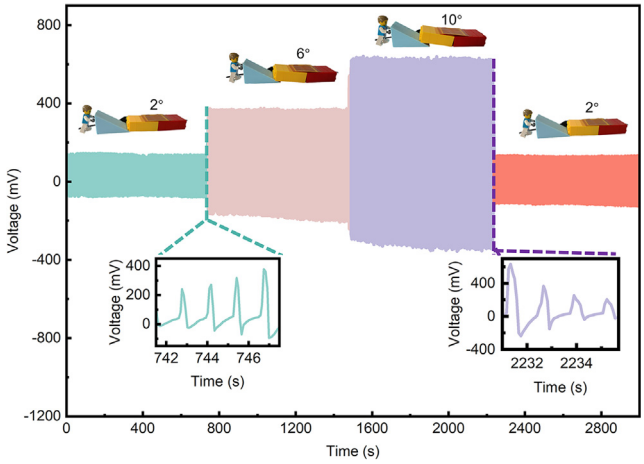

Figure 8. Sensitivity and durability testing of the tilt sensors

the tilt angle generated between the connecting blocks. In addition, the response voltage for the same tilt angle is stable in the continuous tests, indicating that the prepared tilt sensor exhibits excellent stability.

DISCUSSION

In summary, this study prepared the uniformly dispersed BT-PVDF composite films induced by SDS-assisted treatment. The experimental results showed that the distribution of BT particles in the composite films modified by the surfactant are more uniform, the dielectric properties are improved, and the flexoelectric response characteristics are significantly improved. In addition, tilt sensors were fabricated with the uniformly dispersed composite films. It is verified by experiments that the prepared tilt sensor can accurately reflect the change of tilt within small range and that it has strong sensitivity, fast response rate, and excellent stability. This work provides a simple and reliable architectural design for preparing the flexoelectric sensor, suggesting the application potential in the fields of bending sensing and structural health monitoring.

Limitations of the study

This study shows that the dispersion uniformity of nanoparticles can be improved by adding surfactants, the dielectric constant of the composite film could be increased, and a significant flexoelectric effect could be obtained. Based on the research of this paper, we believe that there are still some factors that can affect the flexoelectric effect of the composite film, such as the composition ratio of the composite film and the preparation methods. It may be possible to obtain a more significant flexoelectric effect by optimizing the composition ratio and preparation method. We will continue to explore in future research.

STAR★METHODS

Detailed methods are provided in the online version of this paper and include the following:

- KEY RESOURCES TABLE
- RESOURCE AVAILABILITY
  - Lead contact
  - Materials availability
  - Data and code availability
- EXPERIMENTAL MODEL AND STUDY PARTICIPANT DETAILS
- METHOD DETAILS
  - Preparation of the composite films
  - Characterizations of the composite films
  - Flexoelectric response testing
- QUANTIFICATION AND STATISTICAL ANALYSIS

ACKNOWLEDGMENTS

This work was supported by Zhejiang Provincial Natural Science Foundation (Project No. LGG21E050021), National Natural Science Foundation of China (Project No. 52002150 and 52305059), and the Sci-Tech Planning Project of Jiaxing (Project No. 2020AY10015, 2020AD10015 and 2021AY30020).

AUTHOR CONTRIBUTIONS

Yujie Wei: Methodology; Writing; Data curation. Ying Yu: Conceptualization; Funding acquisition; Writing—review & editing. Yuxin Zuo: Conceptualization. Zhikun Li: Data curation. Zhiqing Gu: Funding acquisition. Hongli Chen: Validation. Yang Yang: Supervision. Chuncheng Zuo: Resources, Supervision.

DECLARATION OF INTERESTS

The authors declare no competing interests.

INCLUSION AND DIVERSITY

We support inclusive, diverse, and equitable conduct of research.

Received: June 16, 2023
Revised: August 8, 2023
Accepted: August 24, 2023
Published: September 9, 2023

REFERENCES

1. Ke, X., Hong, Z., Ma, Q., Wen, X., Wang, Z., Yang, S., Zhang, L., Wang, D., Shu, L., Deng, Q., et al. (2023). Giant flexoelectric coefficients at critical ferroelectric transition. Acta Mater. *245*, 118640. https://doi.org/10.1016/j.actamat.2022.118640.
2. Narvaez, J., Vasquez-Sancho, F., and Catalan, G. (2016). Enhanced flexoelectric-like response in oxide semiconductors. Nature *538*, 219–221. https://doi.org/10.1038/nature19761.
3. Tagantsev, A.K. (1985). Theory of flexoelectric effect in crystals. Sov. Phys. - JETP *61*, 1246. https://doi.org/10.1103/PhysRevB.34.5883.
4. Unnikrishnan, G.K., Sharma, S., Pathak, H., Chauhan, V.S., and Jain, S.C. (2023). Extended Isogeometric Analysis of Cracked Piezoelectric Materials in the Presence of Flexoelectricity. Adv. Theory Simul. *6*, 2200846. https://doi.org/10.1002/adts.202200846.
5. Nirwal, S., Sahu, S.A., Singhal, A., and Baroi, J. (2019). Analysis of different boundary types on wave velocity in bedded piezo-structure with flexoelectric effect. Composites, Part B *167*, 434–447. https://doi.org/10.1016/j.compositesb.2019.03.014.
6. Krishnaswamy, J.A., Rodriguez-Tembleque, L., Melnik, R., Buroni, F.C., and Saez, A. (2020). Size dependent electro-elastic enhancement in geometrically anisotropic lead-free piezocomposites. Int. J. Mech. Sci. *182*, 105745. https://doi.org/10.1016/j.ijmecsci.2020.105745.
7. Liu, K., Shao, S., Ji, H., Wu, T., Shen, S., Zhang, S., and Xu, M. (2022). Enhanced flexoelectricity with pre-strain gradients. Appl. Phys. Lett. *121*, 42904. https://doi.org/10.1063/5.0096936.
8. Hu, X., Zhou, Y., Liu, J., and Chu, B. (2018). Improved flexoelectricity in PVDF/barium strontium titanate (BST) nanocomposites. J. Appl. Phys. *123*, 154101. https://doi.org/10.1063/1.5022650.
9. An, S., Jo, H.S., Li, G., Samuel, E., Yoon, S.S., and Yarin, A.L. (2020). Sustainable Nanotextured Wave Energy Harvester Based on Ferroelectric Fatigue-Free and Flexoelectricity-Enhanced Piezoelectric P(VDF-TrFE) Nanofibers with $BaSrTiO_3$ Nanoparticles. Adv. Funct. Mater. *30*, 1–14. https://doi.org/10.1002/adfm.202001150.
10. Cui, X., Huang, F., Zhang, X., Song, P., Zheng, H., Chevali, V., Wang, H., and Xu, Z. (2022). Flexible pressure sensors via engineering microstructures for wearable human-machine interaction and health monitoring applications. iScience *25*, 104148. https://doi.org/10.1016/j.isci.2022.104148.
11. Wang, Y., Yao, M., Ma, R., Yuan, Q., Yang, D., Cui, B., Ma, C., Liu, M., and Hu, D. (2020). Design strategy of barium titanate/polyvinylidene fluoride-based nanocomposite films for high energy storage. J. Mater. Chem. A *8*, 884–917. https://doi.org/10.1039/c9ta11527g.
12. Ruiz, V.M., Olmos, D., and González-Benito, J. (2023). PVDF/MWCNT nanocomposites with complex configurations prepared by solution blow spinning and their flexoelectric responses. Polymer *267*, 125669. https://doi.org/10.1016/j.polymer.2022.125669.
13. Wang, C., Zhang, Y., Zhang, B., Wang, B., Zhang, J., Chen, L.Q., Zhang, Q., Wang, Z.L., and Ren, K. (2021). Flexophotovoltaic Effect in Potassium Sodium Niobate/Poly(Vinylidene Fluoride-Trifluoroethylene) Nanocomposite. Adv. Sci. *8*, 2004554. https://doi.org/10.1002/advs.202004554.
14. Li, X., Li, Y., and Wu, L. (2020). Enhanced flexoelectricity in $Ba_{0.6}Sr_{0.4}TiO_3$/epoxy composite. Mater. Lett. *260*, 126953. https://doi.org/10.1016/j.matlet.2019.126953.
15. Yan, D., Wang, J., Xiang, J., Xing, Y., and Shao, L.H. (2023). A flexoelectricity-enabled ultrahigh piezoelectric effect of a polymeric composite foam as a strain-gradient electric generator. Sci. Adv. *9*, eadc8845. https://doi.org/10.1126/sciadv.adc8845.
16. Huang, S., Qi, L., Huang, W., Shu, L., Zhou, S., and Jiang, X. (2018). Flexoelectricity in dielectrics: Materials, structures and characterizations. J. Adv. Dielectr. *8*, 1830002. https://doi.org/10.1142/S2010135X18300025.
17. Ehrhardt, C., Fettkenhauer, C., Glenneberg, J., Münchgesang, W., Pientschke, C., Großmann, T., Zenkner, M., Wagner, G., Leipner, H.S., Buchsteiner, A., et al. (2013). $BaTiO_3$-P(VDF-HFP) nanocomposite dielectrics - Influence of surface modification and dispersion additives. Mater. Sci. Eng. B Solid-State Mater. Adv. Technol. *178*, 881–888. https://doi.org/10.1016/j.mseb.2013.04.013.
18. Feng, Y., Peng, C., Deng, Q., Hu, J., Li, Y., and Wu, Q. (2019). Finely depressed dielectric loss and conductivity achieved in high-kappa stannic oxide/polymer nanocomposites from surfactant-assisted electric percolation. J. Mater. Sci. Mater. Electron. *30*, 2682–2692. https://doi.org/10.1007/s10854-018-0544-5.
19. Quqa, S., and Landi, L. (2023). Integrating flexibility-based curvature with quasi-static features induced by traffic loads for high-resolution damage localization in bridges. Mech. Syst. Signal Process. *186*, 109907. https://doi.org/10.1016/j.ymssp.2022.109907.
20. Xu, J., Wei, X., Li, R., Kong, S., Wu, Z., and Wang, Z.L. (2022). A Capsule-Shaped Triboelectric Nanogenerator for Self-Powered Health Monitoring of Traffic Facilities. ACS Mater. Lett. *4*, 1630–1637. https://doi.org/10.1021/acsmaterialslett.2c00477.
21. Zhang, X., Wang, Y., Gao, X., Ji, Y., Qian, F., Fan, J., Wang, H., Qiu, L., Li, W., and Yang, H. (2021). High-Temperature and Flexible Piezoelectric Sensors for Lamb-Wave-Based Structural Health Monitoring. ACS Appl. Mater. Interfaces *13*, 47764–47772. https://doi.org/10.1021/acsami.1c13704.
22. Ghanbari, M., and Yazdanpanah, M.J. (2015). Delay compensation of tilt sensors based on MEMS accelerometer using data fusion technique. IEEE Sensor. J. *15*, 1959–1966. https://doi.org/10.1109/JSEN.2014.2366874.
23. Cai, Y., Yu, C., Ren, Y., Wang, W., Yin, Z., and Xia, C. (2022). High Precision Attitude-Rate Measurement of Magnetically Suspended Control and Sensing Gyroscope Using Variational Mode Decomposition and Wavelet Transform. IEEE Sensor. J. *22*, 1188–1198. https://doi.org/10.1109/JSEN.2021.3131994.
24. Ozioko, O., Nassar, H., and Dahiya, R. (2021). 3D Printed Interdigitated Capacitor Based Tilt Sensor. IEEE Sensor. J. *21*, 26252–26260. https://doi.org/10.1109/JSEN.2021.3058949.
25. Rahman, B.M.A., Brambilla, G., Reduan, S.A., Bayang, L., and Ismail, M.F. (2023). Surface-mounted tilt sensor using fiber Bragg grating technology for engineered slope monitoring with temperature compensation. IEEE Sensor. J. 1–10. https://doi.org/10.1109/JSEN.2023.3268649.

26. Moubarak, P.M., Ben-Tzvi, P., and Zaghloul, M.E. (2012). A self-calibrating mathematical model for the direct piezoelectric effect of a new MEMS tilt sensor. IEEE Sensor. J. *12*, 1033–1042. https://doi.org/10.1109/JSEN.2011.2173188.
27. Byington, C.S., Watson, M.J., Sheldon, J.S., and Swerdon, G.M. (2009). Shaft coupling model-based prognostics enhanced by vibration diagnostics. Insight Non-Destr. Test. Cond. Monit. *51*, 420–425. https://doi.org/10.1784/insi.2009.51.8.420.
28. Mahato, P.K., and Sen, S. (2015). Effect of surface modification of ceramic particles by SDS on the electrical properties of PZT-PVDF and BT-PVDF composites: interface effect. J. Mater. Sci. Mater. Electron. *26*, 2969–2976. https://doi.org/10.1007/s10854-015-2784-y.
29. Tagantsev, A.K., and Yurkov, A.S. (2012). Flexoelectric effect in finite samples. J. Appl. Phys. *112*, 044103. https://doi.org/10.1063/1.4745037.
30. Wang, Q., Zhang, J., Zhang, Z., Hao, Y., and Bi, K. (2020). Enhanced dielectric properties and energy storage density of PVDF nanocomposites by co-loading of $BaTiO_3$ and $CoFe_2O_4$ nanoparticles. Adv. Compos. Hybrid Mater. *3*, 58–65. https://doi.org/10.1007/s42114-020-00138-4.
31. Tabhane, G.H., and Giripunje, S.M. (2020). Robust flower-like ZnO assembled β-PVDF/BT hybrid nanocomposite: Excellent energy harvester. Polym. Test. *88*, 106564. https://doi.org/10.1016/j.polymertesting.2020.106564.
32. Fu, J., Hou, Y., Zheng, M., Wei, Q., Zhu, M., and Yan, H. (2015). Improving Dielectric Properties of PVDF Composites by Employing Surface Modified Strong Polarized $BaTiO_3$ Particles Derived by Molten Salt Method. ACS Appl. Mater. Interfaces *7*, 24480–24491. https://doi.org/10.1021/acsami.5b05344.
33. Zhang, W., Feng, Y., Niu, Y., Liu, T., Zhai, X., and Liu, J. (2021). Surface modification of superfine SiC powders by ternary modifiers-KH560/sodium humate/SDS and its mechanism. Ceram. Int. *47*, 23834–23843. https://doi.org/10.1016/j.ceramint.2021.05.091.
34. Cao, J. (2018). Bioelectricity Inspired Polymer Electrolyte Membranes for Sensing and Engergy Harvesting Applications. http://rave.ohiolink.edu/etdc/view?acc_num=akron1541721597835991.
35. Poddar, S., and Ducharme, S. (2014). Temperature dependence of flexoelectric response in ferroelectric and relaxor polymer thin films. J. Appl. Phys. *116*, 114105. https://doi.org/10.1063/1.4895988.
36. Smith, M., and Kar-Narayan, S. (2022). Piezoelectric polymers: theory, challenges and opportunities. Int. Mater. Rev. *67*, 65–88. https://doi.org/10.1080/09506608.2021.1915935.
37. Bai, P., Zhu, G., Zhou, Y.S., Wang, S., Ma, J., Zhang, G., and Wang, Z.L. (2014). Dipole-moment-induced effect on contact electrification for triboelectric nanogenerators. Nano Res. *7*, 990–997. https://doi.org/10.1007/s12274-014-0461-8.
38. Li, L., Peng, F., Zheng, G., Dai, K., Liu, C., and Shen, C. (2023). Electrospun Core–Sheath PVDF Piezoelectric Fiber for Sensing Application. ACS Appl. Mater. Interfaces *15*, 15938–15945. https://doi.org/10.1021/acsami.2c20512.
39. Kang, S., Kim, S.H., Lee, H.B., Mhin, S., Ryu, J.H., Kim, Y.W., Jones, J.L., Son, Y., Lee, N.K., Lee, K., et al. (2022). High-power energy harvesting and imperceptible pulse sensing through peapod-inspired hierarchically designed piezoelectric nanofibers. Nano Energy *99*, 107386. https://doi.org/10.1016/j.nanoen.2022.107386.

STAR★METHODS

KEY RESOURCES TABLE

REAGENT or RESOURCE	SOURCE	IDENTIFIER
Chemicals, peptides, and recombinant proteins		
barium titanate (BT)	Shanghai Macklin	CAS # 12047-27-7
Polyvinylidene fluoride (PVDF)	Shanghai Macklin	CAS # 24937-79-9
dimethyl sulfoxide (DMSO)	Shanghai Macklin	CAS # 67-68-5
sodium dodecyl sulfate (SDS)	Shanghai Macklin	CAS # 151-21-3
Conductive copper foil tape	3M	N/A
PI tape	3M	N/A
Software and algorithms		
OriginPro 2022	OriginLab	https://www.originlab.com/2022

RESOURCE AVAILABILITY

Lead contact

Further information and requests for resources and reagents should be directed to and will be fulfilled by the lead contact, Ying Yu (yingyu@zjxu.edu.cn).

Materials availability

This study did not generate new unique reagents.

Data and code availability

All data reported in this paper will be shared by the lead contact upon request.
This paper does not report original code.
Any additional information required to reanalyze the data reported in this paper is available from the lead contact upon request.

EXPERIMENTAL MODEL AND STUDY PARTICIPANT DETAILS

This work did not need any unique experimental model.

METHOD DETAILS

Preparation of the composite films

To prepare the composite film, 0.7 g $BaTiO_3$ (barium titanate, BT) was evenly distributed in cathodic surfactant $CH_3(CH_2)_{11}OSO_3Na$ (SDS)-based aqueous solution, and then stirred with a magnetic stir-bar for 120 min at 60°C. Note that the concentration of the SDS modification solution should be kept at the critical micelle concentration of 8.12×10^{-3} M,[28] so that all particles can be functionalized. Then the mixed solution is filtered and washed, and after being dried and ground at 60°C, the SDS-modified BT powder could be obtained. 0.5 g SDS-modified BT powder and polyvinylidene fluoride (PVDF) were dispersed in 5.5 ml dimethyl sulfoxide (DMSO), and magnetically stirred for 120 min at 60°C to obtain a uniform SDS/BT-PVDF precursor solution. In addition, 0.5 g BT and PVDF were added to 5.5 ml of DMSO, and then mixed evenly to form the BT-PVDF precursor solution of the comparison group. The prepared precursor solutions were uniformly poured into glass dishes, and vacuum-dried for 10 h at 60°C to remove the excess solvent to obtain the composite SDS/BT-PVDF films and BT-PVDF films. The thickness of the prepared film was about 0.1mm.

Copper foils were attached on both sides of the composite film as electrodes. After packaging with the insulating PI tape.

Characterizations of the composite films

A scanning electron microscope (SEM, Hitachi SU 8020) was used to study the surface morphology of the composite films. An X-ray diffractometer (XRD, Bruker, D8 Advance) with Cu Kα as the irradiation source (λ = 0.154 nm) and energy-dispersive X-ray spectroscopy (EDS, Ultim Max, Oxford Instruments) detectors with an incident electron beam energy of 300 keV were used to analyze the crystalline structure and elemental distribution, respectively. Zeta potential was tested by Zetasizer Nano analyzer (Malvern, Zetasizer Nano ZS90) with a Universal

'Dip' Cell Kit (Malven, ZEN1002). The dielectric properties of the composite films were tested with a sweep signal from 100 Hz to 1 MHz using an impedance analyzer (WK6505B).

Flexoelectric response testing

The tests of the response characteristics were based on the cantilever beam method. Coaxially connected building blocks were used to simulate the adjacent components in bridges or other structures. The prepared tilt sensor was attached above the junction of the two blocks. Then, a tilt angle α was formed between the two blocks. The response voltage of the tilt sensor was reflected by the KEITHLEY 2450 source meter.

QUANTIFICATION AND STATISTICAL ANALYSIS

The chart shows the average or representative results of multiple independent SEM/electrical experiments. Analyses and plots were performed with OriginPro 2022 software.